NUMERICAL ESTIMATION OF SWIRL AND TUMBLE NUMBERS IN RICARDO RESEARCH ENGINE CYLINDER FOR VARIABLE VALVE LIFTS

S. KARAASLAN[a], E. HEPKAYA[a], N. YÜCEL[a], S.USLU[b]
[a]*Experimental and Computational Combustion Laboratory, Faculty of Engineering, Department of Mechanical Engineering, University of Gazi, 06570 Maltepe-Ankara, TURKEY*
[b]*TOBB University of Economics and Technology, Mechanical Engineering Department, Ankara TURKEY*

Abstract
The turbulence is one of the most important parameters for internal combustion engines. Enough turbulence formations will result in a better mixing process of air and fuel and it will also enhance flame development. The desired turbulent character can be obtained with a well designed intake port. In this study, swirl and tumble motion investigations were performed for Ricardo E6 Research Engine. The CAD model of the engine cylinder with only intake port and intake valve was prepared and imported to STAR- CCM+ v6.04 software. The energy solver was frozen and segregated solver was used during the solutions. The turbulence model selection was a key point for such an analysis. So, three turbulence models (Realizable k-s, k-ro-SST and LES) were compared. The k-s model was found more suitable and stable for these cases. In our investigation, there were two case studies. One of them was effect of valve lift change on swirl and tumble number while the engine was operated constant speed. The second one was effect of engine speed on swirl and tumble number for a unique valve lift. As it is expected for a gasoline engine, the tumble numbers remain higher than swirl numbers. The valve lift change results showed that while increasing of valve lift increased the swirl numbers but decreased the tumble numbers. This inversely proportional result arises from the momentum transform between the angular and axial motions. Anyway, both dimensionless numbers were increased with the engine speed increasing and it was seen that the engine speed is the most effective parameter for incylinder flow formation.

Keywords: Ricardo Engine, Swirl and Tumble Number, CFD Simulation

*Corresponding Author: Tel.: +90 530 974 06 49; Fax: +90 (312) 231 98 10
E-mail Address: karaaslansalih@gazi.edu.tr (S. Karaaslan)

1. Introduction

In order to increase the efficiency of an internal combustion engine, the most important issue is to obtain the optimum thermal efficiency at possible maximum compression ratio. But, if the compression ratio increases too much, the knocking tendency will also increase. To promote rapid combustion, sufficient large-scale turbulence (kinetic energy) is needed at the end of the compression stroke because it will result in a better mixing process of air and fuel and it will also enhance flame development. On the other hand, extremely high turbulence intensity may cause excessive heat transfer from combustion gases to cylinder wall and flame propagation problems [1-3]. So, the most efficient combustion can be obtained in the case of optimum in-cylinder turbulent flow characteristics and these flow characteristics directly depend on design of intake ports [4]. The most important in-cylinder rotating flows are swirl and tumble that occur during intake stroke. While the swirl is the flow around the cylinder axis and the tumble is defined as the flow around the axis perpendicular to the cylinder axis [5].

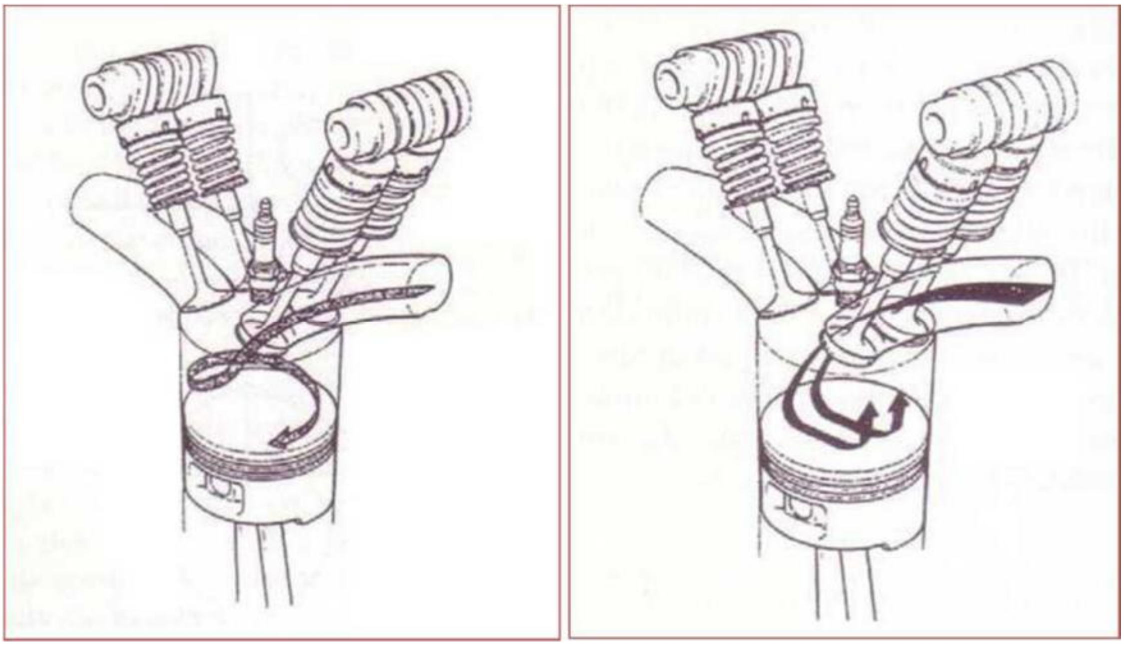

Fig.1 Schematic Representation of Swirl and Tumble Motions in Engine Cylinder.

These flows can be measured experimentally. In the swirl measurement, the air that enters the cylinder from intake port over the valve and rotates the swirl-meter turbine and the turbine gives the swirl characteristics. As in the swirl measurement, tumble flow can be measured by a swirl-meter turbine but this turbine is located the pipes that exit from cylinder wall. These measurements also can be performed using optical accesses. But all these methods are laborious and expensive. So nowadays, this type experiments yield to CFD analyses. At this point, dimensionless swirl and tumble numbers can be estimated by CFD simulations easily and accurately. These numbers define the ratio of angular momentum to axial momentum physically.

Swirl Number:

$$S = \frac{Angular\ Momentum}{Axial\ Momentum} = \frac{\int V_\theta V_z r \rho dA}{\bar{R} \int V_z^2 \rho dA}$$

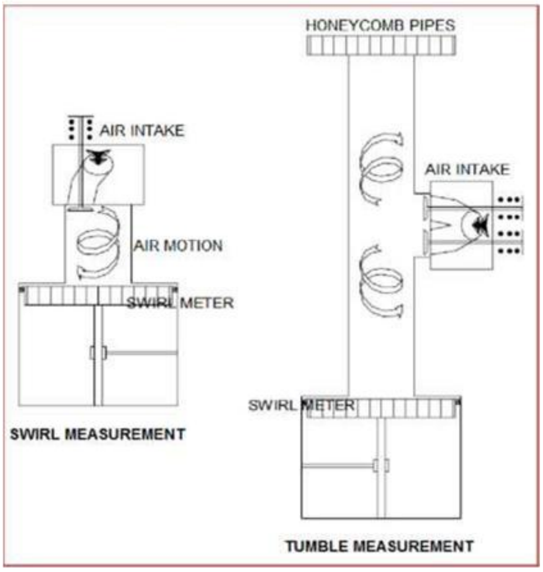

Fig.2 Schematic Representation of Swirl and Tumble Measurement Experiments.

Some experimental and numerical examples of swirl and tumble investigation take part in the literature. Huang et al. [6] have measured in-cylinder flow with PIV method (particle image velocimetry). The engine was single cylinder, four stoke motorcycle engine. Tumble ratio and turbulence intensity was investigated in details for the intake port shape (elliptical and circular). At the intake stroke, both port shapes have given similar results but,

the vortex formation in circular port has disappeared at the compression stroke. The mean tumble ratio and turbulence intensity in elliptical port was higher than circular one. Anyway in performance tests, a performance increase has been monitored for the elliptical port use. Hong and Tarng [7], have investigated the effect of port, valve and cylinder wall structure to the tumble motion experimentally and numerically. A single cylinder, four stroke motorcycle engine have been prepared for optical access and piston have been moved. The turbulent flow field have been measured pint by point with LDV (Laser Doppler Velocimetry). The same engine module has been simulated with KIVA-3V software. Mean velocity, turbulence intensity, tumble ratio, swirl ratio and vortex motions were investigated. Experimental and numerical results were in good agreement. Martins et al. [4], have re-designed the inlet port of a small Internal Combustion Engine in order to enhance the production of turbulence by swirl. To perform this task, Gambit and Fluent was used. Initially the current geometry was tested and proved to create low swirl, so the geometry was changed several times until reaching a good result in terms of generated swirl. The tests include just steady flow, where the air enters the inlet port and leaves the bottom of the cylinder continuously. The flow within the cylinder is examined at specific sections, namely at various heights of the cylinder (horizontal sections) and path lines are also evaluated. The flow is calculated for various valve lifts at a specific engine condition. The swirl numbers around 1 was found suitable for producing required amount of swirl. Payri et al. [8], have performed three-dimensional flow calculations of the intake and compression stroke of a four-valve direct-injection Diesel engine with different combustion chambers. A limited number of validation calculations of the compression stroke were first performed in order to explore the limits of CFD representation of the in-cylinder flow. The calculated flow field in three different combustion chambers was compared with laser Doppler velocimetry measurements; the comparison showed that the three-dimensional model is reasonably accurate for crank-angles around top dead center (TDC). In general, it performed better for low swirl combustion chambers while turbulence velocities are under-predicted when squish effects are important. In the main study, the flow characteristics inside the engine cylinder equipped with different piston configurations were compared. For this, complete calculations of the intake and compression strokes were performed under realistic operating conditions and the ensemble-averaged velocity and turbulence flow fields obtained in each combustion chamber analyzed in detail. The results confirmed that the piston geometry had little influence on the in-cylinder flow during the intake stroke and the first part of the compression stroke. However, the bowl shape plays a significant role near TDC and in the early stage of the expansion stroke by controlling both the ensemble-averaged mean and the turbulence velocity fields. Khalighi et al. [9], have performed multidimensional simulations of coupled intake port/valve and in-cylinder flow structures in a pancake- shape combustion chamber engine are reported. Direct comparisons of three intake configurations for the same cylinder geometry are presented: (1) standard intake valve;
(2) intake valve with high-swirl shroud orientation; and (3) intake valve with across- head shroud orientation. In order to verify the calculated results, qualitative flow visualization experiments were carried out for the same intake geometries during the induction process using a transient water analog. During the intake process the results of the multidimensional simulation agreed very well with the qualitative flow visualization experiments. An important finding in this study was that the standard intake valve configuration (no shroud) generated a well-defined tumbling flow structure at BDC which was sustained and amplified by the compression process and, in turn, caused generation of a high turbulence level before TDC. A comparison between tumble ratios at BDC indicated that in-cylinder tumble was highest for the standard valve intake configuration and lowest for the across-head shroud orientation. Both the standard and high swirl shroud orientation produced the same levels of turbulence during late compression with the across-head shroud orientation being about 30% less.

In this study, a numerical swirl and tumble investigation will be performed for the Ricardo E6 Research Engine with STAR-CCM+ v6.04 software. The engine geometrical specifications are given at Table.1. For the turbulence model selection three models will be tested. Mainly, there are two case studies. One of them is effect of valve lift change on swirl and tumble number while the engine is operated constant speed. The second one is effect of engine speed on swirl and tumble number for a unique valve lift. So, the primary sources of in-cylinder turbulence will be investigated in details numerically.

Table.1 Ricardo E6 Research Engine Geometrical Specifications

Bore	76.2 mm
Stroke	111 mm
Intake Port Diameter	33 mm
Exhaust Port Diameter	28 mm
Intake Valve Diameter	35 mm
Exhaust Valve Diameter	30 mm
Maximum Valve Lift	10 mm

2. Numerical Approach

2.1 Mesh Continuum:

The initial grid distribution of the model surface has coarse tri shaped elements. So firstly, the Surface Remesher option of STAR-CCM+ has been used to resize these surface elements and then, the Polyhedral Mesher method have been chosen for volume meshing. The polyhedral elements are new generation element type. They are preferred because of their capabilities to represent physical geometry well and give more quality elements. The element size used in this study, were chosen with comparative analyses. The specified element sizes were implemented to the model and the change of the maximum velocity values taken from four measurement points were calculated with respect to the element number increase. All mesh study analyses were performed at 2700 rpm engine speed and 10 mm valve lift. These element number and the element number optimization graphs were shown in Table.2.

Table.2 Mesh IDôs and Element Numbers

Mesh ID	Element Number
1	**109811**
2	**218156**
3	**618182**
4	**1154479**
5	**1881774**

Fig.3 Simulation Data Measurement Points.

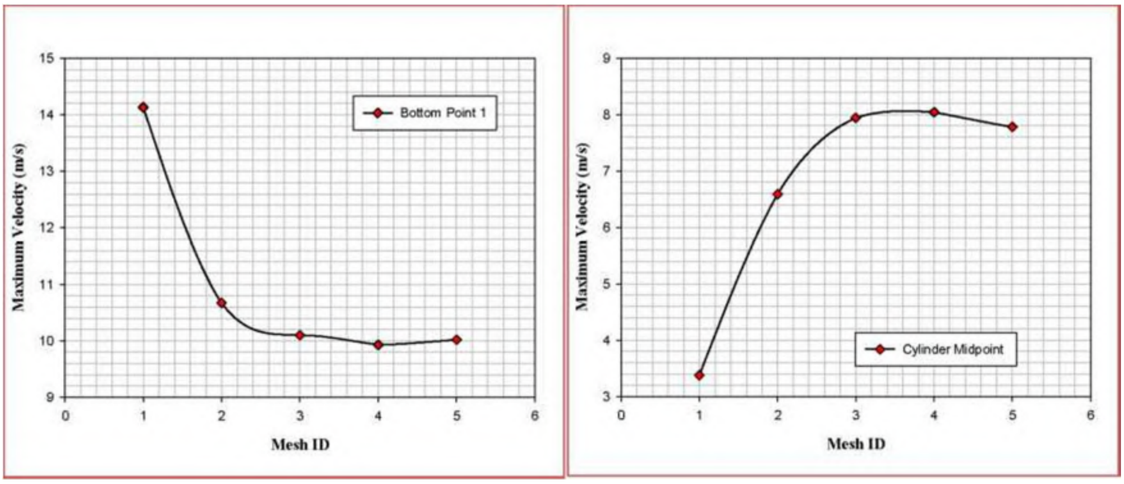

Fig.4a Element Number Optimization Graphs.

Maximum Velocity (m/s)

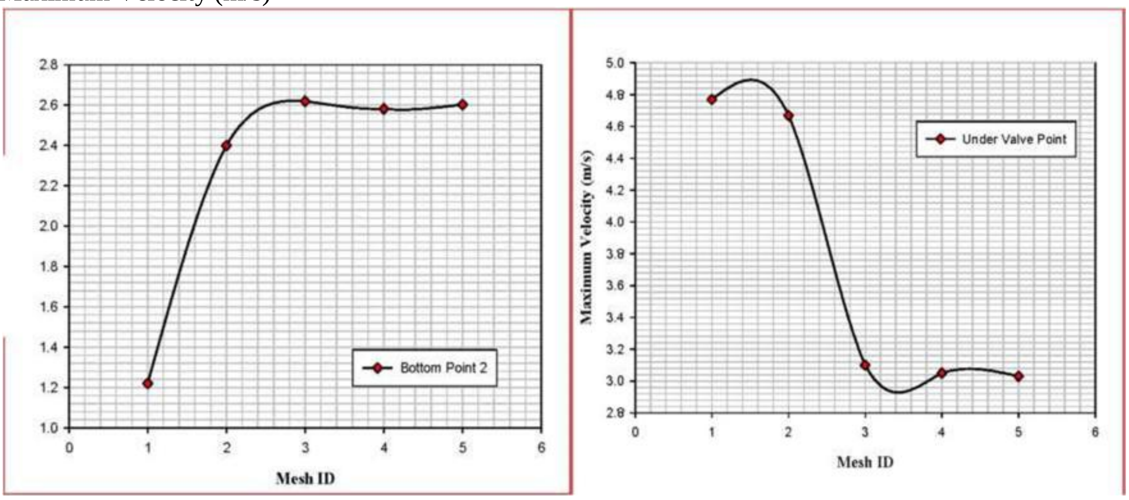

Fig.4b Element Number Optimization Graphs.

As seen from the Fig.4a and Fig.4b, the forth mesh has about 3% -5% deviation according to the third and fifth meshes. This rate was found enough accurate for these analysis and the optimum element number for these cases was 1154479.

Fig.5 Element Distribution of The Continuum.

2.2 Physics Continuum and Solver Settings:

In the simulations, the air was used as the material and it was considered as an ideal gas. During the analyses, the gravitational effects were also enabled. The solver was chosen segregated solver and the energy solver was disabled. Because the calculation was hydrodynamics and the heat transfer was not modeled. The cell quality remediation was preferred in settings to ignore possible cell defects. This option is not a solver option directly. It helps the solver to find defective cells and modifies the results according to the fine cells near. After a steady and an unsteady flow comparison, the time required for being steady was found as 0.5 s physical time and the all other analyses were continued as steady flow. The results of these comparisons are shown in Table.3.

Table.3 Comparison of Steady and Unsteady Simulations Measurement Points (Maximum Velocity Values)

Measurement Points	**Steady**	**Unsteady**
Bottom Point 1	**10.15**	**10.44**
Bottom Point 2	**2.97**	**2.79**
Cylinder Midpoint	**7.198**	**7.09**
Under Valve Point	**3.36**	**3.24**

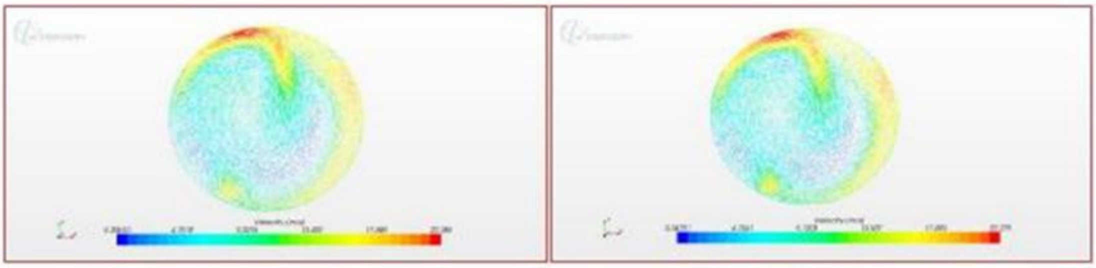

Fig.6 Steady and Unsteady Simulation Results on Midplane of the EngineCylinder.

The swirl and tumble are sensitive and turbulent motions. In order to predict these motions well, directly depend on selected turbulence model. So as a turbulence model, Realizable k-s, k-ro-SST and LES models were tested. The results of tested models shown Table.4.

Table.4 Comparison of Turbulence Models at Measurement Points (Maximum Velocity Values)

Measurement Points	**Realizable k-£**	**k-ra-SST**	**LES**
Bottom Point 1	**10.15**	**9.35**	**9.35**
Bottom Point 2	**2.97**	**3.14**	**5.36**
Cylinder Midpoint	**7.198**	**11.2**	**3.05**
Under Valve Point	**3.36**	**2.63**	**1.62**

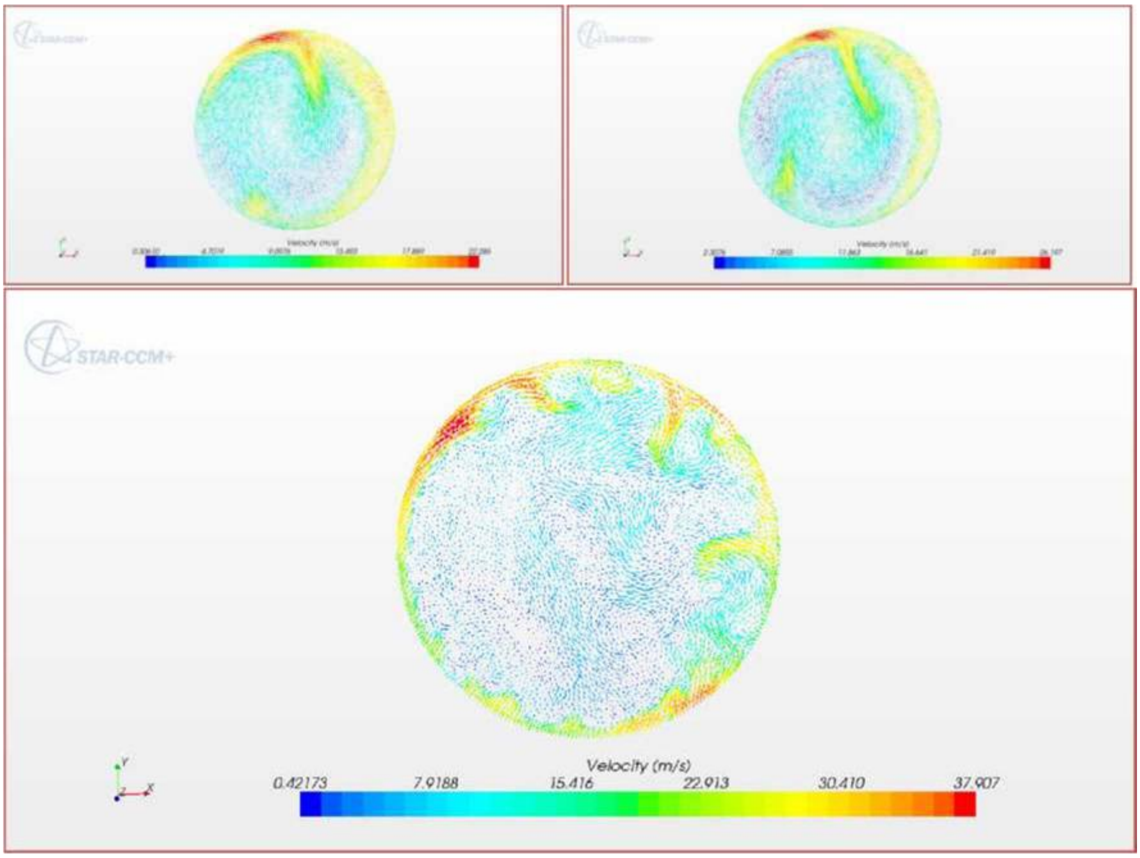

Fig.7 Vector Plot on Midplane of the Engine Cylinder WRT Turbulence Models.

While RANS turbulence models have given relatively to each other, LES model converged and diverged at some measurement points. This fluctuating behavior may cause from the mathematically dependence of the LES model to the cell size. So, the mean turbulence characteristics were more reliable and especially Realizable k-s model was preferred. Because for complex shear flows and highly rotating flows, this model gives more better results than k-ro-SST model.

2.3 Boundary Conditions:

In order to obtain an air velocity at the intake port, the volumetric flow rate can be used depending on engine speed and volumetric efficiency.

$$\dot{Q} = V_D . n . z . \eta_v$$

where;

$n = N/2$ and N = Engine Speed

z = number of cylinders

η_v = volumetric efficiency

Swirl Calculation: At the entrance of intake port, the velocity inlet boundary condition was selected and as in the experiments, the piston head was modeled as pressure outlet (atmospheric condition). All the other faces were assigned as wall.

Tumble Calculation: At the entrance of intake port, the velocity inlet boundary condition was selected and as in the experiments, two pipes have been added to the cylinder wall and their exits were modeled as pressure outlet (atmospheric condition). Piston head and all the other faces were assigned as wall.

3. Results and Discussions:

The calculated swirl and tumble number parameters and the convergence history examples were shown in Fig.8. As seen in residuals graphs, most of the residual values remained under 10^{-} or below. Only the turbulence dissipation rate was higher than the other. This may cause that the flow had extreme rotational motion and this residual value may not converge very fast. But the spot values for specified points were constant totally. So, these convergence criteria were accepted for all the simulations.

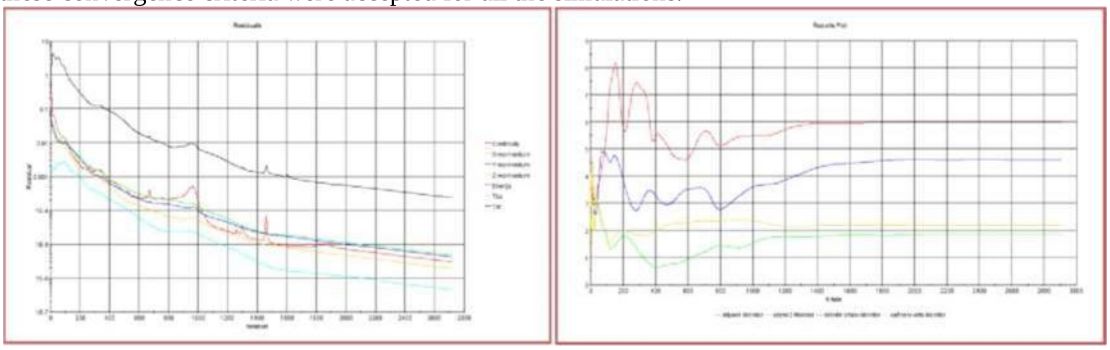

Fig.8 Example Convergence History and Spot Value Graphs.

The change of swirl and tumble numbers with respect to engine speed were shown in Fig.9 At these analyses, constant valve lift (10 mm) was used. The maximum swirl number was about 0.2 and the maximum tumble number was 0.45. The change was nearly linear and this was an expected result. While the engine speed increase, the air velocity will increase too and it will increase the turbulence intensity (Reynolds Number) in the cylinder.

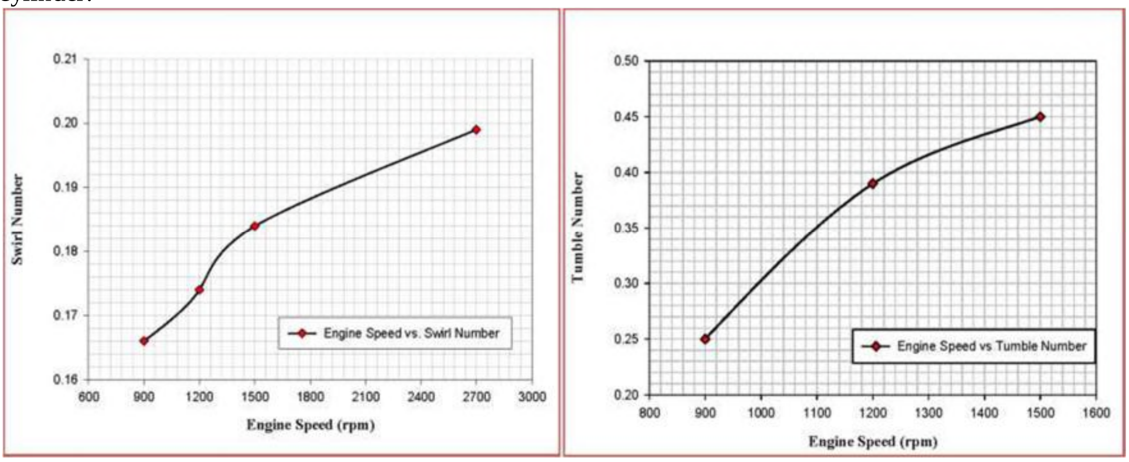

Fig.9 The Change of Swirl and Tumble Numbers WRT Engine Speed.

The change of swirl and tumble numbers with respect to valve lift were shown in figures below. At these analyses, constant engine speed (2700 rpm) was used. The graphs showed that the swirl number increased and the tumble number decreased generally. The maximum swirl number was at 10 mm valve lift with the value of 0.184 and the maximum tumble number was at 2 mm valve lift with the value of 1.07. For the 8 mm lift, both numbers remained different behavior than the others.

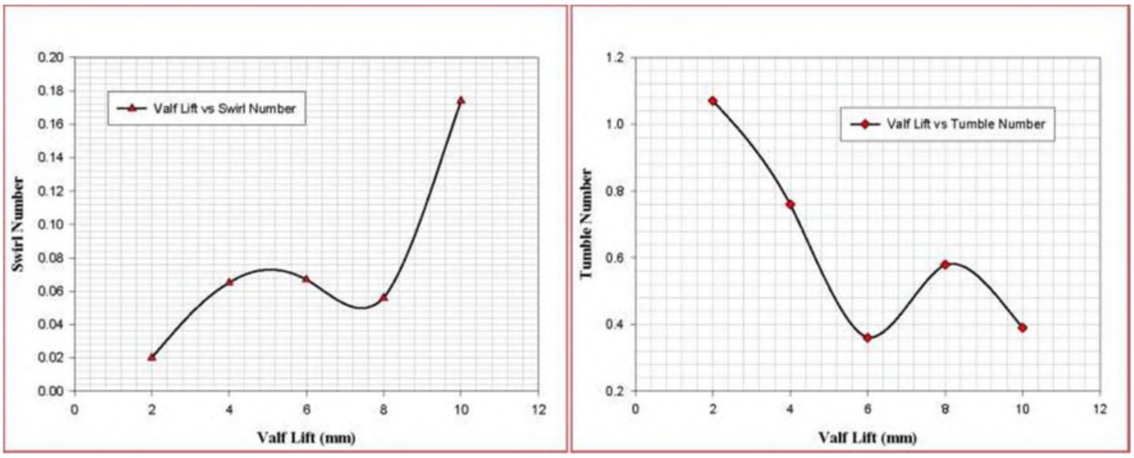

Fig.10 The Change of Swirl and Tumble Numbers WRT Valve Lift.

If the swirl and tumble numbers examined together, there was a inversely proportional case. This case means that increase in axial momentum will increase tumble motion and increase in radial momentum will increase swirl motion. If the conservation of momentum was regarded, the increase of axial momentum will cause decrease in radial momentum and vice versa. So, while swirl number increase, tumble number will decrease too. But still, the tumble numbers will be higher. Because, in gasoline engines primary air motion is tumble and so, it is an expected result for these engine simulations.

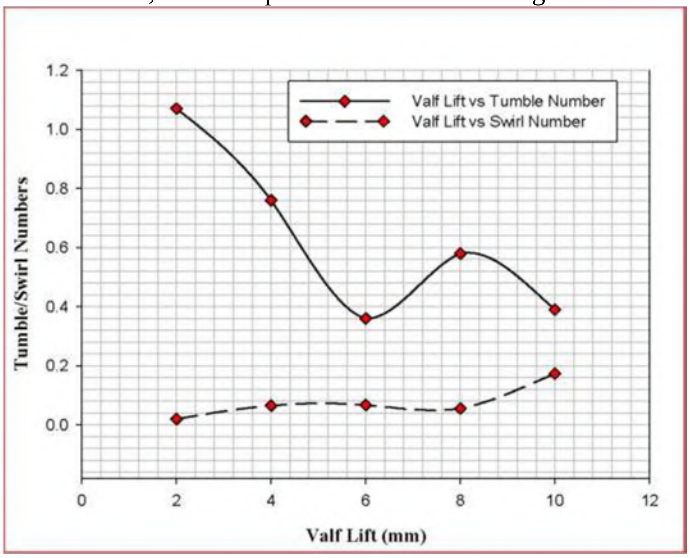

Fig.11 The Comparison of The Change of Swirl and Tumble Numbers WRT Valve Lift.

In the swirl calculation analysis, if the velocity vectors at two different planes are examined, there was a clear difference between 2 mm and 10 mm valve lifts. When the lift value increase, circularity and velocity magnitudes increase. And so, angular momentum and swirl number increase too. But this increase is not extremely and it is not totally important for gasoline engines.

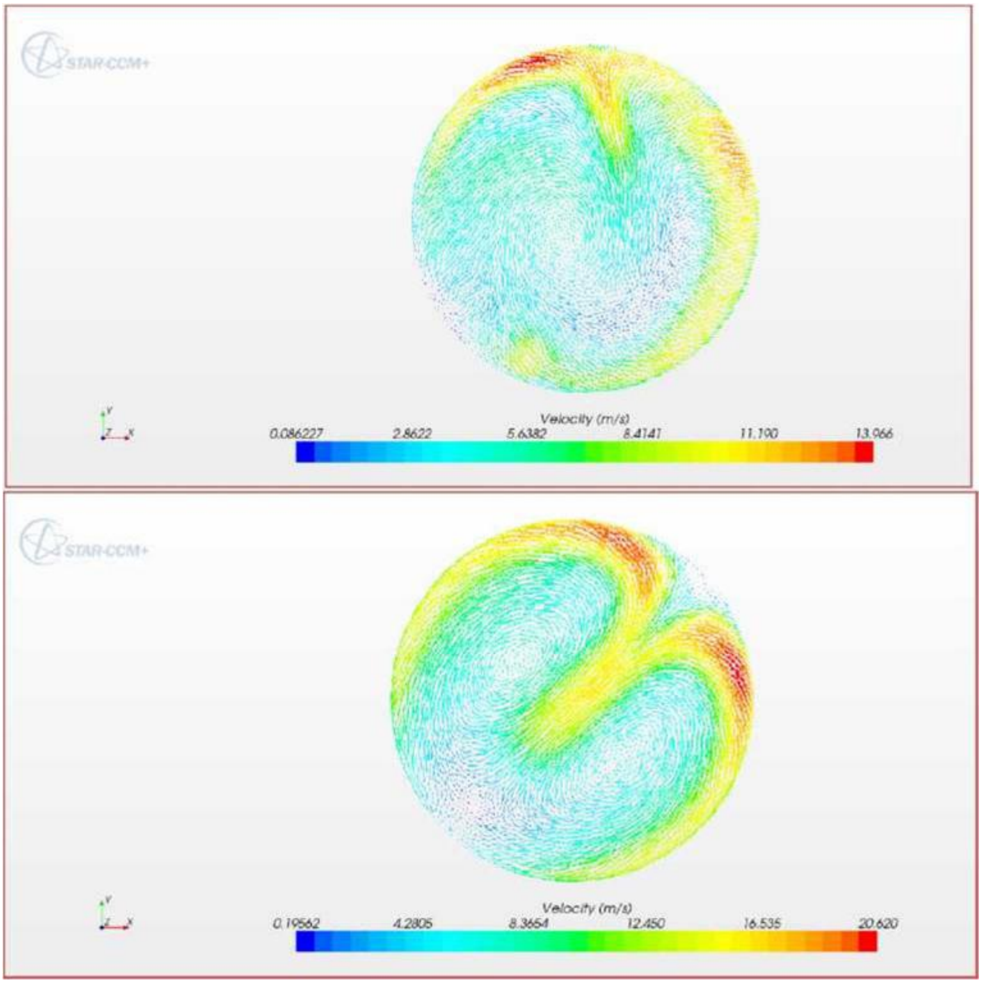

Fig.12 The Vector Plot on Midplane of The Engine Cylinder at 2 mm and 10 mm Valve Lifts, respectively.

In the tumble calculations, 2 mm valve lift has created a nozzle effect and the air velocity has reached to 73 m/s, this high speed air has followed the cylinder walls and entered to the tumble pipe exits directly. When the valve lift increase, the air velocity at the valve seats decrease and for 10 mm valve lift, the air velocity was about 30 m/s. This decrease caused that the air spread more in cylinder volume. So, in the tumble pipes the air velocity was lower than small valve lifts. These lower velocities decrease the rotational flows and increase in axial momentum. Thus while the valve lift increase, the tumble number decrease.

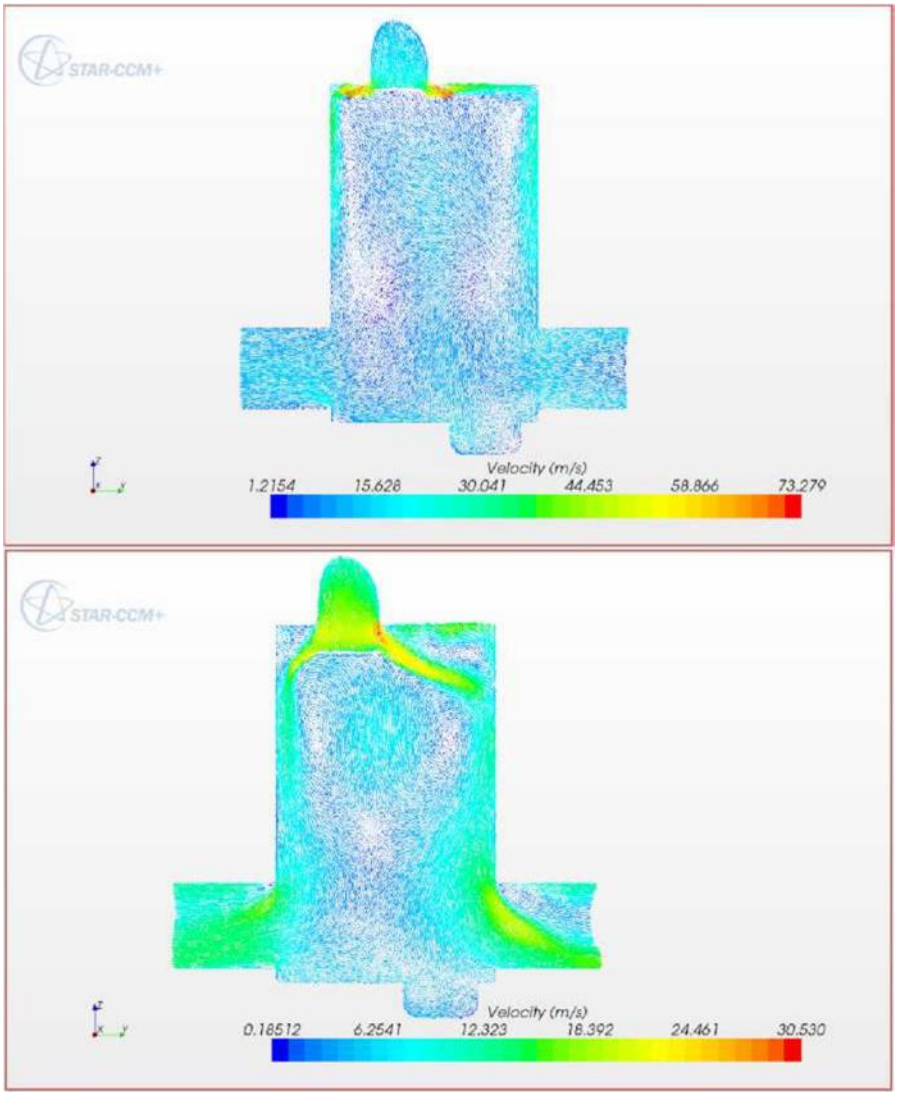

Fig.13 The Vector Plots Represents The Tumble Motion at 2 mm and 10 mm Valve Lifts, respectively.

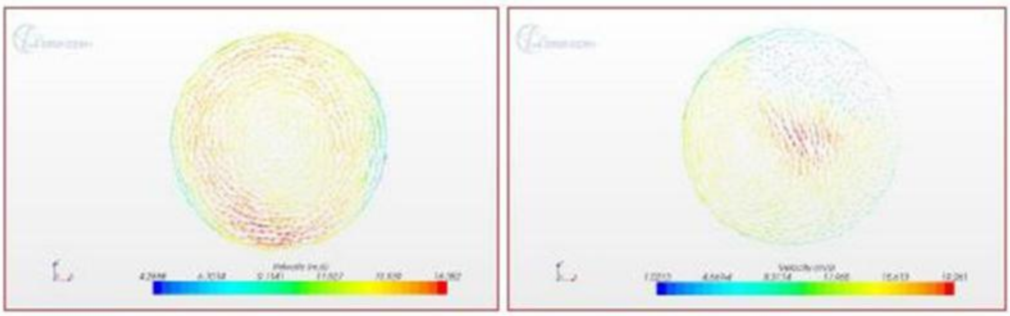

Fig.14 The Vector Plot on Tumble Pipe Planes at 2 mm and 10 mm Valve Lifts, respectively.

4. Conclusion

In the present study, two important in-cylinder air motion: swirl and tumble was investigated numerically. The Intake port, intake valve and cylinder geometry of the Ricardo E6 Research Engine was modeled and the simulations were performed in STAR-CCM+ v6.04 software. The dimensionless parameters swirl and tumble numbers were calculated with respect to engine speed and variable valve lifts. As expected in gasoline engines, the tumble numbers remained higher than swirl numbers. While tumble numbers decreased with the increase of valve lift, swirl numbers had a reverse situation. But for both numbers, the engine speed was a factor of increment. The obtained numerical results gave acceptable turbulent air motion parameters, so in order to get optimum air motion in engine cylinder, new designs can be performed numerically instead of laborious experiments.

5. Acknowledgements

Manuscript received December 28, 2011. This work was supported by the Scientific Technological Research Council of Turkey under Grant of Support Programme for Scientific and Technological Research Project (Project Code: 109M420).

6. References

[1] Blair, G. P. , 1999, Design and Simulation of Four-Stroke Engines, Warrendale (USA), SAE.
[2] Lumley, J. L., 2001, Early work on fluid mechanics in the IC engine, Annual Reviews, Annual Review of Fluid Mechanics Volume 33, Issue 1.
[3] Stone, R. , 1989, Motor Vehicle Fuel Economy, Middlesex (England), Macmillan education LTD.
[4] Martins J., Teixeira S., Coene S., Design of an inlet track of a small IC engine for swirl enhancement, Proceedings of COBEM 2009, 20th International Congress of Mechanical Engineering November 15 20,2009, Gramodo, RS, Brazil.
[5] Lumley JL. Engines - an introduction , Cambridge University Press, 1999.
[6] Huang RF, Lin KH, Yeh CN, Lan J. In-cylinder tumble flows and performance of a motorcycle engine with circular and elliptic intake ports. Exp Fluids (2009) 46:165179.
[7] Hong CW, Tarng SD, In-Cylinder Tumble Flow Field Measurements and Predictions. Journal of Engineering for Gas Turbines and Power, JANUARY 2001, Vol. 123 / 139.
[8] Payri F., Benajes J., Margot X., Gil A., CFD modeling of the in-cylinder flow in direct-injection Diesel engines, Computers & Fluids 33 (2004) 995-1021.
[9] Khalighi, B., Haworth, D., and Huebler, M., "Multidimensional Port-and-in- Cylinder Flow Calculations and Flow Visualization Study in an Internal Combustion Engine with Different Intake Configurations," SAE Technical Paper 941871, 1994, doi:10.4271/941871.